A Simple and Fast Method for the Determination of Lead(II) Ions in Some Cosmetic Products Through Spectrophotometric Technique by Using Thiosemicarbazone-Linked Substituted Indole-2-one

Sulafa Nassar[1], Gharam Ibrahim Mohammed[1], and Thoraya Abdelreheem Farghaly[2*]

[1]*Department of Chemistry, Faculty of Science, Umm Al-Qura University, Makkah 21955, Saudi Arabia*

[2]*Department of Chemistry, Faculty of Science, Cairo University, Giza 12613, Egypt*

* ***Corresponding author:***

email: thoraya-f@cu.edu.eg

Received: September 29, 2025
Accepted: December 12, 2025

DOI: 10.22146/ijc.111616

Abstract: *We aimed to develop a simple, fast, and inexpensive colorimetric approach for detecting lead(II) ions in solution by forming a complex with 1-(1-benzyl-2-oxoindolin-3-ylidene)thiosemicarbazide. A detailed description of spectrophotometric lead(II) determination is provided. When combined with the* N*-benzyl-isatin-thiosemicarbazone ligand (L) in a slightly acidic solution (pH 12), lead(II) produces a yellow chelate. The molar absorptivity of the complex at 253 nm (λ_{max}) is 1.9×10^3 L mol^{-1} cm^{-1}, and the quantification limit is 2.28 μg mL^{-1} (11 μM), whereas the detection limit is 0.73 μg mL^{-1} (3.5 μM). The concentration range when Beer's law is observed is from 9.7×10^{-6} to 1.9×10^{-4} M. We studied the structure and stoichiometry of the Pb(II) and L complex in solution through the synthesis of the solid complex (PbL) and proved using the analytical techniques such as FTIR, NMR, UV-vis spectroscopy, SEM, and thermal analysis. Lead(II) recovery percentages in lipstick samples were determined using the developed method, with results ranging from 88.1 ± 1.9 to 117.3 ± 1.1%. The high lead(II) recovery rate from the samples indicates the effectiveness of the developed method and its potential use for accurate measurement and quality assessment of lead(II) in various samples.*

Keywords: *chemosensor; isatin-thiosemicarbazone ligand; Pb(II); UV-vis spectrum; spectrophotometric technique*

■ INTRODUCTION

Environmental pollution has a detrimental impact on living organisms, particularly humans, by compromising their health and daily functions, leading to numerous diseases [1-3]. This pollution originates from routine activities, including vehicular emissions, tobacco use, and industrial waste. Among the most hazardous pollutants, lead (Pb) is exceedingly harmful to human health, the reproductive system, the central nervous system, the brain, the liver, and wreaks havoc on the kidneys, frequently ending in death. It constitutes a significant environmental pollutant with detrimental health implications for humans [4]. The gradual accumulation of Pb in the human body has an adverse impact on the cardiovascular system, leading to increased mortality rates [5-6]. More than 1.5 million fatalities were attributed to Pb exposure worldwide in 2021, according to the World Health Organization reports [7-8].

In contrast, Pb is integral to many industrial processes, including those that make soldering materials, anti-friction metals, printing metals, Pb-acid storage batteries, and other similar products [9]. Lining tanks and basins in laboratories and insulating wires are two common uses for Pb. Sulfuric acid is made with Pb, which is also commonly found in plumbing systems [10]. One of the most critical materials for nuclear reactor radiation shielding is Pb [11]. Pb poisoning readily occurs via inhalation and ingestion due to its resistance to decomposition and evaporation, unlike other chemicals. Therefore, it is crucial to estimate Pb contents in different media with great precision. Several methods for determining metal concentrations have been rapidly improved and expanded upon, including AAS [12], spectrometry [13-14], voltammetry [15], flow

injection [16], ICP-AES [17], and ICP-MS [18]. The predominant technique is direct visible absorption spectroscopy [19], favored for its convenience [20], rapid methodology [21], cost-effectiveness, reliability, accuracy, availability of equipment, and simplicity of procedure [22-23]. Salicylaldehyde isonicotinoyl hydrazone [24-25], Schiff bases [26], dithizone [27], dimethyl carbonate [28] are among the many ligands that have been reported for metal ion detection using extraction spectrometry. Some disadvantages of these technologies include the need for precise temperature control [29], lengthy extraction times, and interference from particular ions [30-31].

Numerous reports and reviews over the years have shown that thiosemicarbazides serve as valuable intermediates in the synthesis of bioactive compounds and in medicinal chemistry [32-34]. Thiomecarbazone derivatives, particularly those linked to heterocycles, possess nucleophilic atoms such as nitrogen and sulfur, along with other electron-donating atoms in the heterocycles, facilitating coordination bonds in complex formation with diverse metals [35-36]. The combination of isatin analogues with thiosemicarbazones is a promising approach that has attracted interest in the pharmaceutical industry owing to its extensive biological properties and industrial applications [37-39]. Moreover, thiosemicarbazones are classified as "critical ligands" due to their notable binding characteristics, which stem from their thiol-thiol resemblance, allowing them to interact with metal centers in various configurations [40]. Thiosemicarbazone derivatives are highly effective medicinal agents due to their ability to form stable complexes with transition metal ions. The coordination-based detection of various metal ions in water-based solutions relies heavily on thiosemicarbazone [41]. The outstanding chelating (binding) capabilities of this class of chemicals make the usage of the thiosemicarbazone-linked substituted indole-2-one ligand significant. This is expected to provide high sensitivity and selectivity for Pb(II) ions, reducing interference from other metal ions commonly present in cosmetics (such as iron or zinc), a significant problem in trace metal analysis. The goal of this research is to develop a simple, fast, and inexpensive colorimetric approach for detecting and quantifying Pb(II) ions in solution by forming a compound with 1-(1-benzyl-2-oxoindolin-3-ylidene) thiosemicarbazide.

■ EXPERIMENTAL SECTION

Materials

We used analytical-grade ligands and solvents, and followed all instructions carefully. Lead nitrate ($Pb(NO_3)_2$) was sourced from Sigma-Aldrich. All of the glassware was carefully rinsed in HNO_3 (10%) solution (Germany) before use. To prepare a standard solution of Pb(II) ions with a concentration of 4.8×10^{-3} M, 1.59 ± 0.001 g of $Pb(NO_3)_2$ was dissolved and then transferred to a 1 L measuring flask. The flask was then filled up to the mark with ultra-pure distilled water. After that, Pb(II) solutions ranging from 9.7×10^{-6} to 1.9×10^{-4} M were diluted with water to create new solutions. To prepare the ligand (L) stock solution, 100 mL of dimethyl sulfoxide (DMSO, Hayman, England) was mixed with an appropriate weight (0.1 ± 0.001 g). The pH was adjusted using NaOH (0.2 M) [42]. A combination of CH_3COOH, H_3PO_4, and H_3BO_3 (0.12 M) was used to generate a severe Britton-Robinson (B-R) buffer with a pH range of 3–12.

Instrumentation

A Shimadzu UV-1800 UV-vis spectrophotometer was used to record the absorbance values of the L and its Pb(II) complex. The instrument had quartz cells and a bath length of 1 cm. The diluted solutions were made using a 10–1,000 µL digital micro-pipette (Volac), and the pH meter (a Mettler Toledo MP220) was used to alter the pH of the solutions. An FTIR spectrophotometric instrument, the Bruker Tensor 27, was used for the measurements. Thermogravimetric analysis (TGA) of the Pb(II) complex was conducted in a nitrogen atmosphere using a Shimadzu DTG-60 model apparatus, at a rate of 10 °C/min, with temperatures increasing from room temperature to 800 °C.

Procedure

Synthesis of L

We subjected a mixture of 20 mL of pure ethanol, 0.5 mL of HCl, and an equal number of moles (5 mmol)

of *N*-benzyl isatin and thiosemicarbazide to microwave irradiation at 110 °C under pressure conditions with an 800 W power output for 30 min in an HP-500 process vial. The yellow *N*-benzyl-isatin-thiosemicarbazone (L) was successfully synthesized using standard procedures (Scheme 1) and subsequently recrystallized from ethanol, yielding 94% of the product. The m.p. 148–150 °C [43]; The M.f./M.wt ($C_{16}H_{14}N_4OS$/310.37 g mol^{-1}): Anal. Calc. (Found) C, 61.92 (61.83); H, 4.55 (4.39); N, 18.05 (17.92); FTIR ν (cm^{-1}): 3451 (N–H), 3084 (C–H sp^2), 1735 (C=O), 1590 (C=N), 1452, 1333, 1270 (C=S).

Synthesis of Pb(II) complex (PbL)

Firstly, 2 mmol of L was mixed with 20 mL of boiling dioxane to create the Pb(II) complex of L. Then, 2 mmol of $Pb(NO_3)_2$ dissolved in distilled water was added dropwise and refluxed for 2 h. Inducing the formation of the solid complex required adding 2 mL of Et_3N to the reaction mixture and allowing it to reflux for 1 h. Anhydrous $CaCl_2$ was used to dry the orange solid under vacuum after filtering, rinsing three times with ether, and so on. The Pb-complex was produced as [L-Pb(NO_3)] with a relatively low yield of 45%. Molecular weight: 578.57, with the following percentages: C, 33.21 (33.03), H, 2.26 (2.12), N, 12.10 (12.05), Pb, 35.81 (35.57), and S, 5.54 (5.39). The following FTIR data are shown in cm^{-1}, KBr disc: 3494 (br. NH_2), 1720 (C=O), 1580 (C=N), 1450–1350 (br., NO_3), 812 (M–S), 682 (M–N).

Application

For the calibration curve, 10 mL volumetric flasks were filled with a precise amount of L (3.2×10^{-3} M) and the appropriate amounts of Pb(II) solutions (from 9.7×10^{-6} to 1.9×10^{-4} M). After adding 2.0 mL of 0.2 M NaOH to the pH-adjusted solutions, 10 mL of distilled water was added. The complex's absorbance at 253 nm was compared to that of the L blank after 5 min of resting the solution combinations at room temperature.

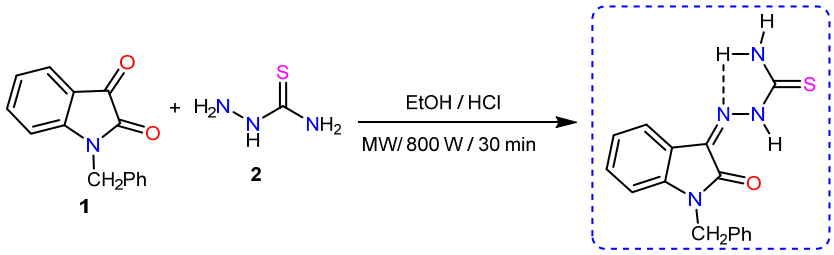
Lipstick samples for analysis were typically prepared by involving acid digestion to break down the organic matrix and dissolve the target analytes. HNO_3 is a commonly used acid, often in combination with others, due to its strong oxidizing properties. Then, 0.5 g of lipstick was taken from each sample and transferred to a beaker. A mixture of 5 mL of concentrated acids, consisting of HNO_3 and HCl in a 3:1 ratio, was added to the lipstick samples for 2 h on a hot plate [44]. To obtain a clear solution, the digested samples were diluted in 10 mL of triple-distilled water and filtered through filter paper. Finally, the suggested approach performed a Pb quantification study on the resultant clear solution.

■ RESULTS AND DISCUSSION

The Characterization of L and Pb(II) Complex

We produced and separated the solid Pb(II) complex to investigate the L-Pb(II) interaction sites. In the solution phase, we verified the stoichiometric ratio of the L to Pb(II). Multiple spectroscopic methods were employed to confirm the L's structure, including FTIR spectroscopy (Fig. S1). This method revealed that the NH and NH_2 groups exhibited a broad absorption band at 3451 cm^{-1}, while the C=N and C=S groups showed strong absorption bands at 1590 and 1270 cm^{-1}, respectively. In addition, Fig. S2 for the ^{1}H-NMR spectrum showed a singlet signal for the CH_2 of the *N*-benzyl group at 4.98 ppm, along with three more singlet signals for the three NH protons at 8.76, 9.10, and 12.42 ppm for the NH_2 and NH groups, and nine protons from the two aromatic rings, anywhere from 7.03 to 7.73 ppm.

Additional evidence to support the hypothesized structure of the newly created complex was provided by



Scheme 1. Synthesis of L

analyzing and comparing the IR spectra between the L and PbL complex. A change from 3451 cm^{-1} to a higher value of 3494 cm^{-1} in the absorption band for the NH and NH_2 groups suggests that the free NH_2 group in the complex is having an effect. When the C=N band shifted from 1590 cm^{-1} in L to 1580 cm^{-1} in the complex, it was established that the Pb(II) metal ion bound to the nitrogen of the C=N group [36]. When the C=S band at 1270 cm^{-1} is absent from the complex, it means that the C=S group has transformed into a thiol group. This new group then forms a covalent bond with the Pb(II) metal ion at 812 cm^{-1}, as indicated by the M–S bond [45]. Detection of a broad band at 1450–1350 cm^{-1} for the NO_3 group, it is likely that a bond has formed between it and the metal ion [46]. Also, the NMR spectrum of the complex reveals a singlet signal for NH_2 at 10.15 ppm and a downfield shift of the CH_2 group from 4.98 ppm (L) to 5.19 ppm (complex), which further supports the coordination between Pb(II) and L, along with the three NH singlet signals in L, for each of the nine protons in the complex, aromatic protons impacted by coordination between Pb and L were detected at 6.79–7.37 ppm.

To illustrate the breakdown process for the Pb(II) complex, we examined the TGA and TDA curves (Fig. S3). The Pb(II) complex was heated under nitrogen from 20 to 900 °C at a rate of 10 °C/min. The Pb(II) complex combination degraded in three distinct phases, as seen by the TGA curve. Decomposition rates of 23.42% for NO_2 and 23.67% for $PhCH_2$ were recorded during the first stage, which began at 37.11 °C and ended at 364.82 °C. A 3.48% (3.62%) loss of the NH_2 group was the outcome of the second stage, which took place between 365.61 and 679.97 °C. Near the computed figure of 9.587%, the last step at temperatures ranging from 681.15 to 901.72 °C showed a loss of N_3 (9.86%). Based on the information provided, the structure of the Pb(II) complex may be determined as [L-Pb(NO_3)], where each ligand is reduced to 1 Pb in the presence of an anion NO_3.

In most cases, the organic and inorganic compounds can be better understood by examining SEM images of these compounds [47]. SEM of L showed a needle cluster at a 50 μm size. Fig. 1 shows that the surface appears to be covered with thick needles measuring approximately 100 μm. In contrast, a cluster

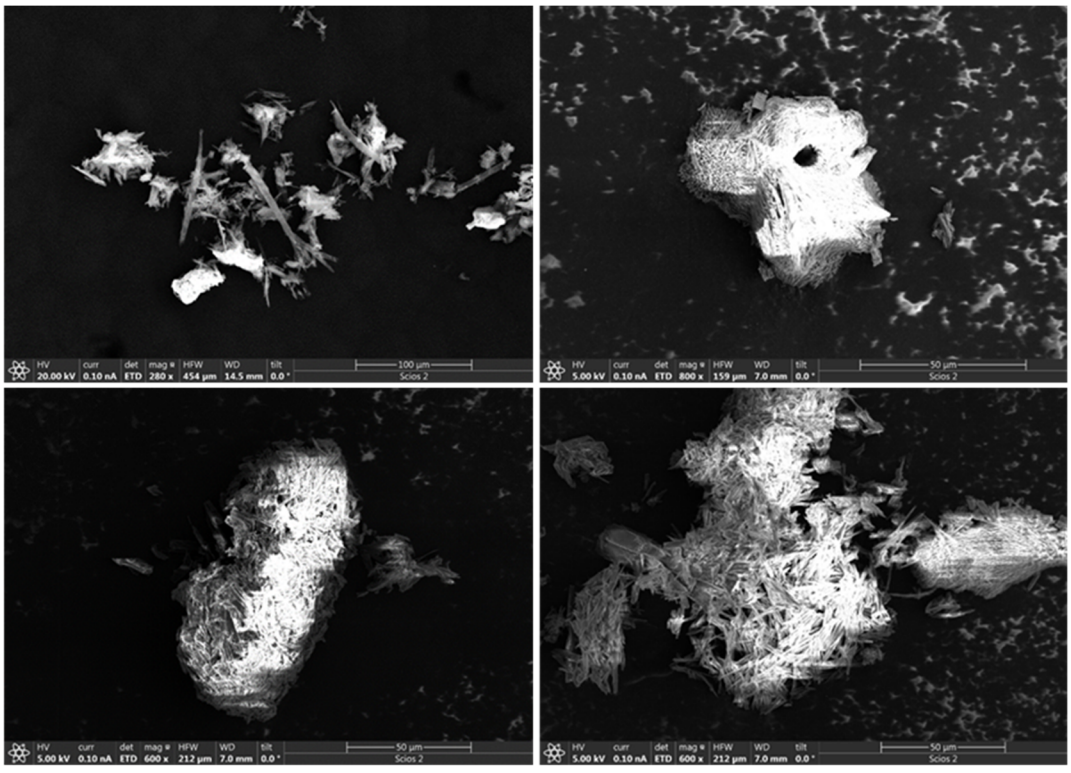


Fig 1. The SEM image of L

of sheets resembling a flower developed on the surface of the Pb(II) complex (Fig. 2). This stood in stark contrast to the L's surface form. The SEM image of the Pb(II) complex showed an increase in surface area, which can enhance its reactivity.

Because L's electronic spectra showed a clearly defined peak at 403 nm and an unclear peak at 265 nm (resembling a shoulder), the $\pi \rightarrow \pi^*$ transitions were consistently assigned to them. With a pH of 12 (0.2 M NaOH), L forms a complex with Pb(II), which causes a change in hue from white to light yellow. The absorption spectrum of the Pb(II) complex (Fig. 3) showed a peak at 253 nm, which was attributed to ligand-to-metal charge transfer (LMCT) [48].

Analytical Parameter Optimization

The development of metal complexes relies heavily on pH control. The effects of pH in the 2.0–12.0 range were investigated using B-R buffer. A stable and maximal absorbance signal was only achieved at pH 12. Stronger coordination to Pb(II) is encouraged by the significant deprotonation of several common donor groups at pH 12, which also increases L basicity and the number of accessible anionic donor sites. Since a constant pH of 12 was shown to be optimal, a further experimental study was conducted to assess the impact of basicity. Utilizing concentrations of ranging from 0.1 to 1.0 M, the effect of hydroxide ion concentration was investigated. The results of this study are presented in Fig. 4. We observed that the absorbance reached its peak at 0.2 M NaOH.

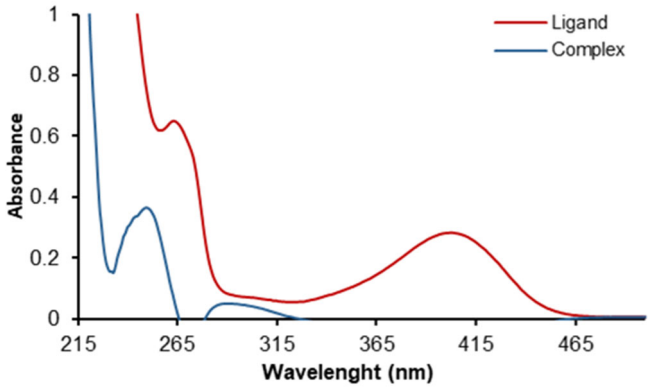


Fig 3. Absorption spectra of 6.4×10^{-5} M of L and 9.7×10^{-5} M of Pb(II) complex in 0.2 M NaOH at 253 nm

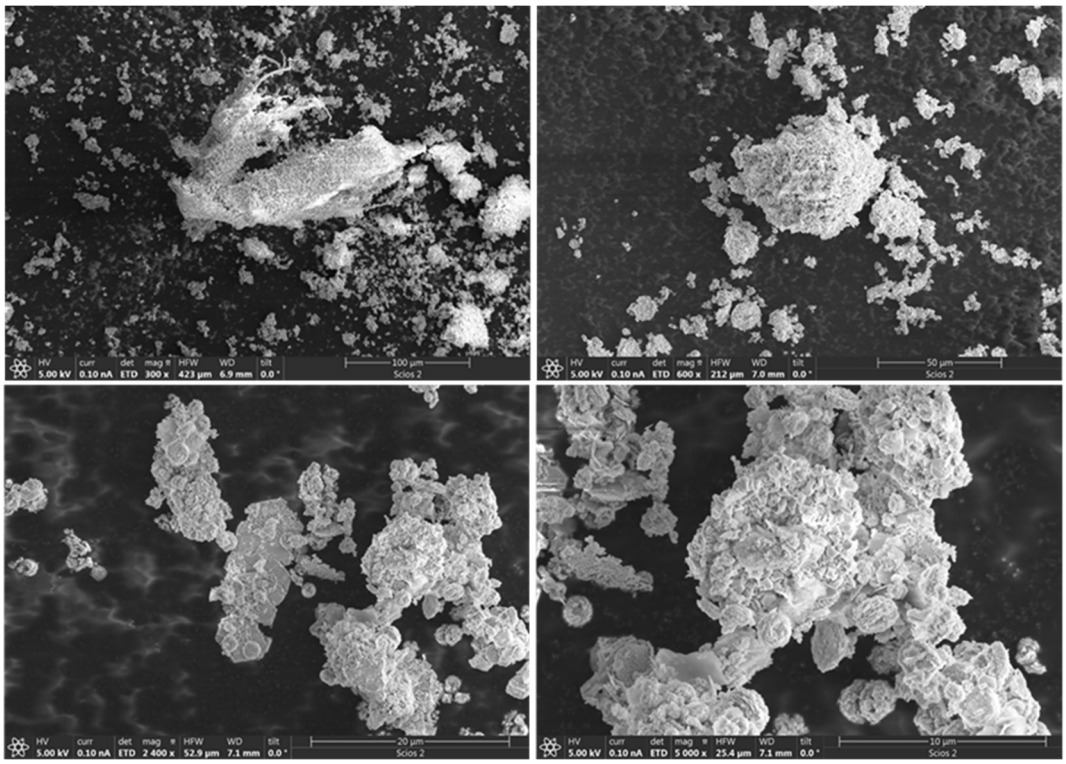


Fig 2. The SEM image of Pb(II) complex

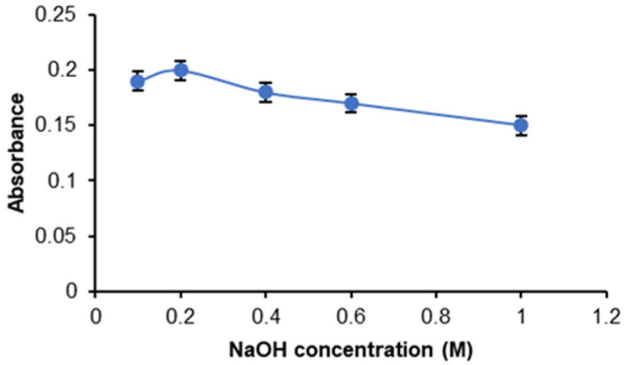


Fig 4. Basicity impact on absorbance of 9.7×10^{-5} M of Pb(II) complex in 6.4×10^{-5} M of L at 253 nm

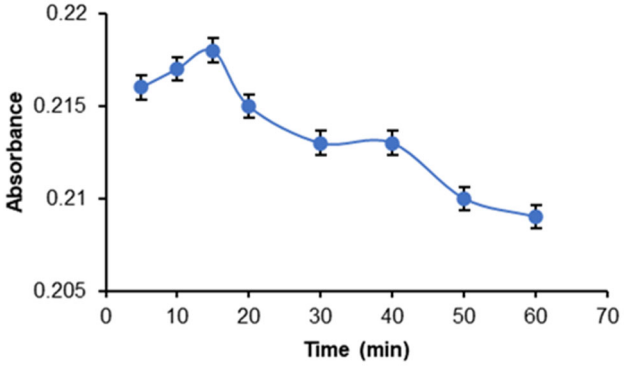


Fig 5. Plot of the PbL complex absorbance over time from 9.7×10^{-5} M Pb(II) solution with L (6.4×10^{-5} M) at 253 nm in 0.2 M NaOH

At various time intervals ranging from 5 to 60 min, the complex stability created was tested in an optimal analytical environment. The complex's absorbance peaked after 15 min of development, as illustrated in Fig. 5. Spectra were captured throughout this period, further supporting the interaction between the Pb(II) and L.

This investigation examined the effect of L concentration on the absorbance of a Pb(II) complex. With the addition of 0.2 M NaOH, a range of concentrations from 6.4×10^{-6} to 9.6×10^{-5} M was introduced to the Pb(II) solution. Despite the broad peak, the Pb(II) complex attained its maximum absorbance at 6.4×10^{-6} M (0.02 mL, 0.1% w/v) of L. The optimal L concentration was found to be 6.4×10^{-5} M (0.2 mL, 0.1% w/v) due to the sharpness and clarity of the peak. Additionally, temperature is a crucial and intricate element in the formation and stability of coordination complexes. We examined the effects of a temperature range of 20–50 °C on complex formation. The Pb(II) complex becomes less stable as the temperature increases. The optimal temperature was 20 °C.

Analytical Performance

To evaluate the efficacy of the proposed approach under the previously defined ideal conditions, the approach relied on L forming a bright yellow complex with Pb(II) ions in an aqueous medium. Fig. 6 displays the absorption spectra, computed under the previously indicated ideal circumstances, of the Pb(II) complex at various concentrations of Pb(II) ions, ranging from 9.7×10^{-6} to 1.9×10^{-4} M. A plot of the Pb(II) complex absorbance at 253 nm vs. Pb(II) concentration confirmed that the Lambert-Beer law was followed.

Fig. 7 shows that within the concentration range of 9.7×10^{-6} to 1.9×10^{-4} M, a linear relationship exists between the absorbance of the produced Pb(II) complex

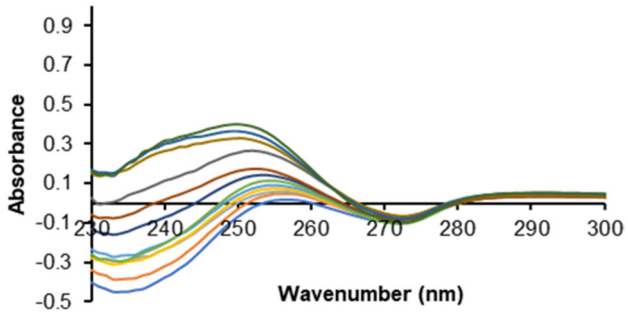


Fig 6. The electronic profiles of the absorbance of the Pb(II) complex at 253 nm at various concentrations of Pb(II) (9.7×10^{-6}–1.9×10^{-4} M) in the presence of L (6.4×10^{-5} M) in 0.2 M NaOH

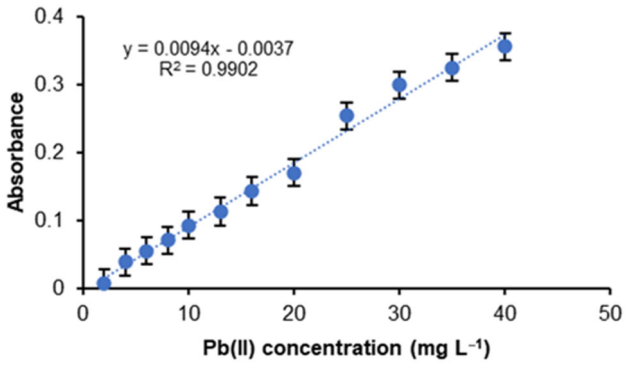


Fig 7. Calibration curve of PbL complex at optimum conditions: [Pb(II)] = 9.7×10^{-6}–1.9×10^{-4} M in 6.4×10^{-5} M L in 0.2 M NaOH at 253 nm

at 253 nm and the concentration of Pb(II) ions, with a correlation coefficient of 0.9902. Eq. (1) represents the linear plot.

$$A = 0.0094\ C\ (M) + 0.0037 \quad (R^2 = 0.9902) \tag{1}$$

The Lambert-Beer line indicated that the Pb(II) complex had a molar absorptivity of $1.9 \times 10^3\ M^{-1}\ cm^{-1}$.

The analytical method's sensitivity was examined using limit of detection (LOD) and limit of quantification (LOQ) values. Based on the calibration curve, LOD and LOQ were determined using Eq. (2) and (3) [49];

$$LOD = \frac{3\sigma}{S} \tag{2}$$

$$LOQ = \frac{10\sigma}{S} \tag{3}$$

where S is the response's standard deviation, and σ is the slope of the calibration curve. The LOD and LOQ values, which were $2.28\ \mu g\ mL^{-1}$ (11 μM) and $0.73\ \mu g\ mL^{-1}$ (3.5 μM), respectively, are listed in Table 1 under optimal analytical conditions for Pb(II) complex synthesis. An accuracy of 0.23% (n = 6) was determined by calculating the RSD, which stands for the relative standard deviation. As indicated in Table 2, the obtained data were compared with alternative methods [50-54] in several analytical characteristics, including LOD, LOQ, and RSD%.

Stoichiometry of Pb(II) Complex

This Pb(II) complex was shown to have the correct stoichiometry using the molar-ratio method. The data confirmed a 1:1 Pb(II)-to-L stoichiometry. Ions of Pb(II) are chelated with L at a concentration of 1 mol. We determined the stability constant of the colored Pb(II) complex at pH 12 using the molar-ratio method [55]. A_{extp}, the total absorbance of the Pb(II) complex, is located close to the equivalence point on the molar ratio plot. Fig. 8 shows how the complex's 1:1 (Pb:L) ratio stoichiometry is utilized using Eq. (4);

Table 1. Quantitative factors for determining the Pb(II) complex

Parameters	Values
pH	12
λ_{max}	253 nm
Molar ratio (Pb:L)	1:1
Beer's law limits ($\times 10^{-5}$ M)	9.7×10^{-6}–1.9×10^{-4}
Molar absorptivity ($M^{-1}cm^{-1}$)	1.9×10^3
Regression equation	A = 0.0094C + 0.0037
Intercept	0.0037
Slope	0.0094
Correlation coefficient (R^2)	0.9902
RSD%	0.23%
LOD ($\mu g\ mL^{-1}$)	0.73
LOQ ($\mu g\ mL^{-1}$)	2.28

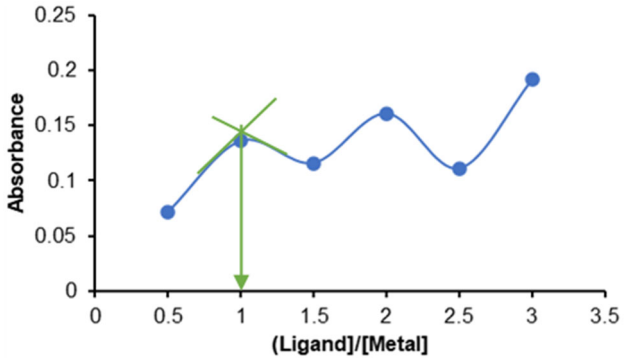


Fig 8. Molar ratio plot for PbL complex formation at 3.2×10^{-3} M of both Pb(II) and L solutions in 0.2 M NaOH at 253 nm

Table 2. Comparison of the recommended method with the currently reported Pb(II) determination technique

Method	RSD%	LOD	LOQ ($\mu g\ L^{-1}$)	Matrix	Ref.
Inductively coupled plasma/optical emission spectroscopy	-	125.14 mg L^{-1}	379.23	Drilling-fueled soil	[50]
Graphite furnace atomic absorption spectroscopy	5	0.188 μg L^{-1}	-	Milk	[51]
Fluorescence	8	4.2×10^{-4} mg kg^{-1}	-	Bee products	[52]
Laser-induced breakdown spectroscopy	3.5	0.028 mg/kg		Cosmetics	[53]
Anodic stripping voltammetry	7.87	11.5 μg L^{-1}	38.2	Wastewater sample from the battery industry	[54]
UV-vis	0.23	0.73 μg L^{-1}	2.28	Lipstick samples	Curr. study

Table 3. Analysis of Pb(II) in a lipstick sample by the developed method

Sample	Pb(II) added (μg mL^{-1})	Pb(II) found (μg mL^{-1})[a]	Recovery (%)[b]
Lipstick 1	0.0	15.0 ± 0.10	–
	8.0	23.8 ± 0.12	110.0 ± 2.5
	20.0	38.5 ± 0.20	117.3 ± 1.1
Lipstick 2	0.0	30.0 ± 0.06	–
	8.0	38.3 ± 0.07	104.0 ± 1.4
	20.0	47.6 ± 0.11	88.1 ± 1.9

[a] Average of measurements ± standard deviation (n = 5)
[b] Average of recovery ± relative standard deviation (n = 5)

$$M^{n+} + X \rightleftharpoons [MX]^{n+} \quad (4)$$

where the L is represented by X and Pb(II) ions are denoted by M^{n+}. [MX] is calculated using Eq. (5);

$$\frac{A}{A_{extp}} = \frac{[MX]^{n+}}{C} \quad (5)$$

where Pb(II) represents the entire analytical concentration, and C stands for L. Hence, Eq. (6–8) are used to find the concentration of MX.

$$[MX] = \frac{A}{A_{extp}} C \quad (6)$$

$$[M]^{n+} = C_m - [MX]^{n+} = C_m - \frac{A}{A_{extp}} C \quad (7)$$

$$[X] = C_x - [MX]^{n+} = C_x - \frac{A}{A_{extp}} \quad (8)$$

To find the stability constant (K) of the generated complex, one might use Eq. (9).

$$K = \frac{[MX]}{[M][X]} \quad (9)$$

The computed value of the stability constant is 2.90×10^{1} mol^{-1} L.

Analytical Applications

The new method was tested using Pb(II) measurement in lipstick samples. Lipstick samples were spiked with different concentrations of Pb(II) (4.0–20.0 mg/L) and then evaluated using the previously established method, as shown in Table 3. Pb(II) recovery percentages in lipstick samples ranged from 88.1 ± 1.9 to 117.3 ± 1.1%.

■ CONCLUSION

A new chemosensor for detecting Pb(II) ions in water samples has been developed using a spectrophotometric approach. A stable chelate with L at a pH of 12 formed the basis of the novel technique. At λ = 253 nm, a complex absorption was observed. In the concentration range of 9.7×10^{-6} to 1.9×10^{-4} M, a linear relationship was observed with a R^2 of 0.9902. The LOQ and LOD were 2.28 and 0.73 μg mL^{-1}. By comparing the outcomes of Job's molar-ratio techniques, we can determine that the complex has a 1:1 stoichiometric composition of M:L. Additionally, we have recovered the solid complex that is formed when L interacts with Pb and have used other analytical approaches to explore its structure. Pb(II) recovery percentages in lipstick samples were determined using the developed method, with results ranging from 88.1 ± 1.9 to 117.3 ± 1.1%. The high Pb(II) recovery rate from the samples indicates the effectiveness of the developed method and its potential use for accurate measurement and quality assessment of Pb(II) in various samples.

■ CONFLICT OF INTEREST

The authors declare that they have no known competing financial interests or personal relationships that could have appeared to influence the work reported in this paper.

■ AUTHOR CONTRIBUTIONS

Sulafa Nassar: Methodology, Investigation, Formal analysis, Software, Resources, Data curation, Writing – original draft. Gharam Ibrahim Mohammed: Investigation, Formal analysis, Writing – review & editing, Writing – original draft, Software, Resources. Thoraya Abdelreheem Farghaly: Synthesis of the ligand,

Writing – original draft, Writing – review & editing. All authors read and agreed to the final version of this manuscript.

■ REFERENCES

[1] Wang, Y., Zhang, Z., Hao, Z., and Eriksson, T., 2025, Environmental regulation and mental well-being: Evidence from China's air pollution prevention and control action plan, *Soc. Sci. Med.*, 365, 117584.

[2] Scimeca, M., Palumbo, V., Giacobbi, E., Servadei, F., Casciardi, S., Cornella, E., Cerbara, F., Rotondaro, G., Seghetti, C., Scioli, M.P., Montanaro, M., Barillà, F., Sisto, R., Melino, G., Mauriello, A., and Bonfiglio, R., 2024, Impact of the environmental pollution on cardiovascular diseases: From epidemiological to molecular evidence, *Heliyon*, 10 (18), e38047.

[3] Zhang, L., Ma, R., Yang, L., Zhang, X., and He, H., 2024, Impact of environmental pollution on ant (*Camponotus japonicus*) development and labial gland disease, *J. Hazard. Mater.*, 477, 135360.

[4] Mansoor, H.S., Salman, T.A., and Dhahir, S.A., 2025, Synthesis of titanium dioxide nanoparticles for removal of Pb^{2+}, Cd^{2+} and Cr^{3+} from wastewater, *Indones. J. Chem.*, 25 (5), 1350–1360.

[5] Collin, M.S., Venkatraman, S.K., Vijayakumar, N., Kanimozhi, V., Arbaaz, S.M., Stacey, R.G.S., Anusha, J., Choudhary, R., Lvov, V., Tovar, G.I., Senatov, F., Koppala, S., and Swamiappan, S., 2022, Bioaccumulation of lead (Pb) and its effects on human: A review, *J. Hazard. Mater. Adv.*, 7, 100094.

[6] Huang, H., Guan, H., Tian, Z.Q., Chen, M.M., Tian, K.K., Zhao, F.J., and Wang, P., 2024, Exposure sources, intake pathways and accumulation of lead in human blood, *Soil Secur.*, 15, 100150.

[7] WHO, 2024, *Lead Poisoning*, World Health Organization, Geneva, Switzerland, https://www.who.int/news-room/fact-sheets/detail/lead-poisoning-and-health, accessed on 24 July 2025.

[8] Boskabady, M., Marefati, N., Farkhondeh, T., Shakeri, F., Farshbaf, A., and Boskabady, M.H., 2018, The effect of environmental lead exposure on human health and the contribution of inflammatory mechanisms, a review, *Environ. Int.*, 120, 404–420.

[9] McKeon, B.B., Furukawa, J., and Fenstermacher, S., 2014, Advanced lead–acid batteries and the development of grid-scale energy storage systems, *Proc. IEEE*, 102 (6), 951–963.

[10] Chowdhury, S., Kabir, F., Mazumder, M.A., and Zahir, M.H., 2018, Modeling lead concentration in drinking water of residential plumbing pipes and hot water tanks, *Sci. Total Environ.*, 635, 35–44.

[11] Kanagaraj, B., Anand, N., Raj, S., and Lubloy, E., 2024, Advancements and environmental considerations in Portland cement-based radiation shielding concrete: Materials, properties, and applications in nuclear power plants– review, *Cleaner Eng. Technol.*, 19, 100733.

[12] Inobeme, A., Mathew, J.T., Jatto, E., Inobeme, J., Adetunji, C.O., Muniratu, M., Onyeachu, B.I., Adekoya, M.A., Ajai, A.I., Mann, A., Olori, E., Akhor, S.O., Eziukwu, C.A., Kelani, T., and Omali, P.I., 2023, Recent advances in instrumental techniques for heavy metal quantification, *Environ. Monit. Assess.*, 195 (4), 452.

[13] Llaver, M., Oviedo, M.N., Quintas, P.Y., and Wuilloud, R.G., 2021, "Analytical Methods for the Determination of Heavy Metals in Water" in *Remediation of Heavy Metals*, Eds. Inamuddin, I., Ahamed, M.I., Lichtfouse, E., and Altalhi, T., Springer International Publishing, Cham, Switzerland, 1–50.

[14] Demir, C., Öner, M., Çetin, G., and Bakırdere, S., 2024, A simple and effective graphene oxide-zinc oxide nanocomposite based solid phase extraction method for the determination of cadmium in tea matrix at trace levels by flame atomic absorption spectrophotometry, *J. Food Compos. Anal.*, 127, 105968.

[15] Deswati, D., Suyani, H., Safni, S., Loekman, U., and Pardi, H., 2013, Simultaneous determination of cadmium, copper and lead in sea water by adsorptive stripping voltammetry in the presence of calcon as a complexing agent, *Indones. J. Chem.*, 13 (3), 236–241.

[16] Kagaya, S., Hida-Matsuda, K., Tsuzaka, S., Minami, C., Gemmei-Ide, M., Cattrall, R.W., and Kolev,

S.D., 2023, The determination of zinc using flow injection and continuous flow analysis combined with a polymer inclusion film-coated column: Application to the determination of zinc in alloys and commercial lithium chloride, *Talanta*, 259, 124545.

[17] Hussain, M.N., Khudhair, A.F., Ahmed, H.J., 2024, Evaluation of lead ion in the wastewater of the lifting and treatment stations using ICP-MS and CPE methods, *Indones. J. Chem.*, 24 (3), 715–728.

[18] Alhagri, I.A., Al-Hakimi, A.N., Al-Hazmy, S.M., and Albadri, A.E.A.E., 2024, Determination of trace and heavy metals in bottled drinking water in Yemen by ICP-MS, *Results Chem.*, 8, 101558.

[19] Alzahrani, L., El-Ghamry, H.A., Saber, A.L., and Mohamed, G.I., 2023, Spectrophotometric determination of mercury(II) ions in laboratory and Zamzam water using bis Schiff base ligand based on 1,2,4-triazole-3,5-diamine and *o*-vaniline, *Arabian J. Chem.*, 16 (1), 104418.

[20] Carter, J.B., Huffaker, R., Singh, A., and Bean, E., 2023, HUM: A review of hydrochemical analysis using ultraviolet-visible absorption spectroscopy and machine learning, *Sci. Total Environ.*, 901, 165826.

[21] Li, X., Qiu, H., Ding, A., and Fan, P., 2025, Heavy metal concentrations prediction of marine sediments by visible-near infrared spectroscopy based on attention mechanism, *J. Hazard. Mater.*, 484, 136729.

[22] Bar, N., Chowdhury, P., and Kanti Das, G., 2024, The photodynamic approach to the molecular-level origin of metal-guided photochromism and ultrafast absorption spectroscopy, *Spectrochim. Acta, Part A*, 312, 124031.

[23] Fakayode, S.O., Bolton, B., Dassow, B., Galvez, K., and Chohan, H., 2024, Rapid screening and multicomponent quantifications of active components of oral syrup over-the-counter medications by Raman and UV–visible spectroscopy and multivariate regression analysis, *Spectrochim. Acta, Part A*, 305, 123447.

[24] Jansová, H., Kubeš, J., Reimerová, P., Štěrbová-Kovaříková, P., Roh, J., and Šimůnek, T., 2018, 2,6-Dihydroxybenzaldehyde analogues of the iron chelator salicylaldehyde isonicotinoyl hydrazone: Increased hydrolytic stability and cytoprotective activity against oxidative stress, *Chem. Res. Toxicol.*, 31 (11), 1151–1163.

[25] Ji, Y., Dai, F., and Zhou, B., 2018, Designing salicylaldehyde isonicotinoyl hydrazones as Cu(II) ionophores with tunable chelation and release of copper for hitting redox Achilles heel of cancer cells, *Free Radical Biol. Med.*, 129, 215–226.

[26] More, M.S., Joshi, P.G., Mishra, Y.K., and Khanna, P.K., 2019, Metal complexes driven from Schiff bases and semicarbazones for biomedical and allied applications: A review, *Mater. Today Chem.*, 14, 100195.

[27] Nur, Y., Rohaeti, E., and Darusman, L.K., 2017, Optical sensor for the determination of Pb^{2+} based on immobilization of dithizone onto chitosan-silica membrane, *Indones. J. Chem.*, 17 (1), 7–14.

[28] Lorêdo de França, M., Separovic, L., Longo Junior, L.S., de Oliveira, D.C., Rebello Lourenço, F., and Calixto, L.A., 2021, Determining uncertainty in a simple UV–vis spectrometry method employing dimethyl carbonate as green solvent for lead determination in water, *Measurement*, 173, 108581.

[29] Singh, A., Shah, S.S., Sharma, C., Gupta, V., Sundramoorthy, A.K., Kumar, P., and Arya, S., 2024, An approach towards different techniques for detection of heavy metal ions and their removal from waste water, *J. Environ. Chem. Eng.*, 12 (3), 113032.

[30] Mandal, S., and Lahiri, S., 2022, A review on extraction, preconcentration and speciation of metal ions by sustainable cloud point extraction, *Microchem. J.*, 175, 107150.

[31] Malik, L.A., Bashir, A., Qureashi, A., and Pandith, A.H., 2019, Detection and removal of heavy metal ions: A review, *Environ. Chem. Lett.*, 17 (4), 1495–1521.

[32] Abdelbaki, H., Djemoui, A., Ouahrani, M.R., Messaoudi, M., Ben Amor, I., Alsaeedi, H., Cornu, D., Bechelany, M., and Barhoum, A., 2025, Synthesis of bioactive 1,4-disubstituted 1,2,3-triazole-linked Thiosemicarbazone derivatives using Cu_2O microbeads catalysis for enhanced

antibacterial and antioxidant activities, *J. Mol. Struct.*, 1324, 140784.

[33] Farghaly, T.A., Masaret, G.S., and Abdulwahab, H.G., 2024, Novel 1,3-indanedione-thiazole hybrids as small-molecule SARS-COV-2 main protease inhibitors with potential anti-coronaviral activity, *Polycyclic Aromat. Compd.*, 44 (10), 6941–6956.

[34] Farghaly, T.A., Al-Hasani, W.A., Ibrahim, M.H., Abdellattif, M.H., and Abdallah, Z.A., 2023, Design, synthesis, anticancer activity and docking studies of thiazole linked phenylsulfone moiety as cyclin-dependent kinase 2 (CDK2) inhibitors, *Polycyclic Aromat. Compd.*, 43 (6), 5001–5020.

[35] Cebotari, D., Builș, J., Garbuz, O., Balan, G., Marrot, J., Guérineau, V., Touboul, D., Haouas, M., Segado-Centelles, M., Bo, C., Gulea, A., and Floquet, S., 2023, A new series of bioactive $Mo^{(V)}_2O_2S_2$-based thiosemicarbazone complexes: Solution and DFT studies, and antifungal and antioxidant activities, *J. Inorg. Biochem.*, 245, 112258.

[36] El-Ghamry, H.A., Fawzy, A., Farghaly, T.A., Bawazeer, T.M., Alqarni, N., Alkhatib, F.M., and Gaber, M., 2022, Evaluation of the efficiency of divalent cobalt and copper chelates based on isatin derivatives and thiosemicarbazide ligands as inhibitors for the corrosion of Sabic iron in acidic medium, *Arabian J. Chem.*, 15 (1), 103522.

[37] Haribabu, J., Alajrawy, O.I., Jeyalakshmi, K., Balachandran, C., Krishnan, D.A., Bhuvanesh, N., Aoki, S., Natarajan, K., and Karvembu, R., 2021, *N*-substitution in isatin thiosemicarbazones decides nuclearity of Cu(II) complexes – Spectroscopic, molecular docking and cytotoxic studies, *Spectrochim. Acta, Part A*, 246, 118963.

[38] Balachandran, C., Haribabu, J., Jeyalakshmi, K., Bhuvanesh, N.S.P., Karvembu, R., Emi, N., and Awale, S., 2018, Nickel(II) bis(isatin thiosemicarbazone) complexes induced apoptosis through mitochondrial signaling pathway and G0/G1 cell cycle arrest in IM-9 cells, *J. Inorg. Biochem.*, 182, 208–221.

[39] Yuan, Q., Cheng, R., Zou, S., Ding, C., Liu, H., Wang, Y., Yang, D., Xiao, X., Jiang, Q., Tang, R., and Chen, J., 2020, Isatin thiosemicarbazone derivatives as inhibitors against corrosion of AA6060 aluminium alloy in acidic chloride medium: Substituent effects, *J. Mater. Res. Technol.*, 9 (5), 11935–11947.

[40] Hazani, N.N., Mohd, Y., Sheikh Mohd Ghazali, S.A.I., Farina, Y., and Dzulkifli, N.N., 2019, Electrochemical studies on corrosion inhibition behaviour of synthesised 2-acetylpyridine 4-ethyl-3-thiosemicarbazone and its tin(IV) complex for mild steel in 1 M HCl solution, *J. Electrochem. Sci. Technol.*, 10 (1), 29–36.

[41] Prajapati, N.P., and Patel, H.D., 2019, Novel thiosemicarbazone derivatives and their metal complexes: Recent development, *Synth. Commun.*, 49 (21), 2767–2804.

[42] Vogel, A.I., 1966, *A Text-Book of Quantitative Inorganic Analysis, Including Elementary Instrumental Analysis*, Longmans, London, UK.

[43] Haribabu, J., Subhashree, G.R., Saranya, S., Gomathi, K., Karvembu, R., and Gayathri, D., 2016, Isatin based thiosemicarbazone derivatives as potential bioactive agents: Anti-oxidant and molecular docking studies, *J. Mol. Struct.*, 1110, 185–195.

[44] Alqahtani, A.M., Mojally, M., Sayqal, A., Ainousah, B.E., Alqmash, A., Alzahrani, S., Alqurashi, G., Wawi, O., and Alsharif, A., 2024, Determination of lead and cadmium concentration in cosmetic products in the Saudi market, *J. Umm Al-Qura Univ. Appl. Sci.*, 10 (1), 146–155.

[45] Takroni, K.M., Farghaly, T.A., Harras, M.F., and El-Ghamry, H.A., 2020, Synthesis, structure elucidation, DNA binding and molecular docking studies of novel copper(II) complexes of two 1,3,4-thiadiazolethiosemicarbazone derivatives, *Appl. Organomet. Chem.*, 34 (10), e5860.

[46] Hashemi, L., and Morsali, A., 2011, Sonochemical synthesis of nano-structured lead(II) complex: Precursor for the preparation of PbO nano-structures, *J. Coord. Chem.*, 64 (23), 4088–4097.

[47] Al-Fahemi, J.H., Saad, F.A., El-Metwaly, N.M., Farghaly, T.A., Elghalban, M.G., Saleh, K.A., and Al-Hazmi, G.A., 2017, Synthesis of Co(II), Cu(II), Hg(II), UO_2(II) and Pb(II) binuclear nanometric

complexes from multi-donor ligand: Spectral, modeling, quantitative structure–activity relationship, docking and antitumor studies, *Appl. Organomet. Chem.*, 31 (11), e3787.

[48] Lever, A.B.P., 1984, *Inorganic Electronic Spectroscopy*, Elsevier, Amsterdam, Netherland.

[49] Miller, J.N., and Miller, J.C., 2009, *Statistics and Chemometrics for Analytical Chemistry*, Pearson/Prentice Hall, Harlow, Essex, UK.

[50] Rehan, I., Gondal, M.A., and Rehan, K., 2018, Determination of lead content in drilling fueled soil using laser induced spectral analysis and its cross validation using ICP/OES method, *Talanta*, 182, 443–449.

[51] Mehrasebi, M.R., Peyda, M., Feizolahi, R., Taromi, A., Homayuni, P., Fathi, S., and Farahmandkia, Z., 2023, Comparison of three digestion methods for determination of lead and cadmium in milk and dairy products, *Environ. Health Eng. Manage. J.*, 10 (2), 191–196.

[52] Talio, M.C., Acosta, M., and Fernández, L.P., 2025, Determination of lead in bee products by solid surface fluorescence using complexation and coacervation at room temperature processes. An environmental friendly methodology, *J. Fluoresc.*, 35 (3), 1611–1623.

[53] Liu, Y., Chu, Y., Hu, Z., Zhang, S., Ma, S., Khan, M.S., Chen, F., Zhang, D., Guo, L., and Lau, C., 2020, High-sensitivity determination of trace lead and cadmium in cosmetics using laser-induced breakdown spectroscopy with ultrasound-assisted extraction, *Microchem. J.*, 158, 105322.

[54] Bedin, K.C., Mitsuyasu, E.Y., Ronix, A., Cazetta, A.L., Pezoti, O., and Almeida, V.C., 2018, Inexpensive bismuth-film electrode supported on pencil-lead graphite for determination of Pb(II) and Cd(II) ions by anodic stripping voltammetry, *Int. J. Anal. Chem.*, 2018 (1), 1473706.

[55] Sawyer, D.T., Heinemann, W.R., Beebe, J.M., and Reilley, C.N., 1984, *Chemistry Experiments for Instrumental Methods*, John Wiley & Sons, Hoboken, NJ, US.